

## NEWS

OF THE NATIONAL ACADEMY OF SCIENCES OF THE REPUBLIC OF KAZAKHSTAN  
PHYSICO-MATHEMATICAL SERIES

ISSN 1991-346X

<https://doi.org/10.32014/2019.2518-1726.70>

Volume 6, Number 328 (2019), 25 – 33

UDC 524.7, 524-1:629.78

IRSTI 41.27.29, 89.51.17

**K. Boshkayev<sup>1,2,3</sup>, G. Zhumakhanova<sup>2</sup>, K. Mutalipova<sup>2</sup>, M. Muccino<sup>4</sup>**<sup>1</sup>NNLOT, <sup>2</sup>Al-Farabi Kazakh National University, Almaty, Kazakhstan;<sup>3</sup>Department of Physics, Nazarbayev University, Nur-Sultan, Kazakhstan;<sup>4</sup>INFN, Laboratori Nazionali Di Frascati, Frascati, Italy[kquantay@mail.ru](mailto:kquantay@mail.ru), [zhumakhanova@gmail.com](mailto:zhumakhanova@gmail.com),[kalbinur.mutalipova@mail.ru](mailto:kalbinur.mutalipova@mail.ru), [marco.muccino@lnf.infn.it](mailto:marco.muccino@lnf.infn.it)**INVESTIGATION OF DIFFERENT DARK MATTER PROFILES**

**Abstract.** Different, commonly accepted and widely used phenomenological dark matter profiles such as the pseudo-isothermal sphere, Burkert, Navarro-Frenk-White, Moore and Einasto profiles are employed to estimate the mass distribution of dark matter in various galaxies. The Newtonian gravity is involved to perform computations at large galactic scales. The distribution of dark matter in diverse types of galaxies is assumed to be spherical without taking into account the complex structure of galaxies such as their cores, inner and outer bulges, disks and halos. The theoretical rotation curves are overlapped with the observations for each individual galaxy. By means of the least square algorithm the model parameters are inferred from the observational data and are subjected to the Bayesian information criterion, which identifies the more preferred model. The masses of dark matter are calculated for each galaxy, with all listed profiles, and compared with the visible masses of the galaxies. The results are in agreement with the ones in the literature.

**Keywords:** galaxies, rotation curves, dark matter.

**Introduction**

Astronomers face the fundamental problem of a mass deficiency, which is known as the dark matter (DM) problem at galactic scales. One observes the presence of DM from dynamical astronomical measurements, but up to now no one was able to detect any DM particle yet in the ground based laboratories. The only knowledge we possess is the fact that DM interacts with an ordinary matter via gravity and dominates preferentially on large scales. It is therefore of particular importance to understand its properties to set guidelines in preparing more focused physics experiments to detect it. The determination of the mass distribution in galaxies is one of the most basic subjects in galactic astronomy, and is usually obtained by analyzing rotation curves.

The idea of DM does not alter the law of gravity like Modified Newtonian Dynamics [1], but proposes that there exists a new type of matter that has yet to be identified. This idea is also supported by gravitational lensing experiments [2]. DM does not participate in electromagnetic and strong interactions; otherwise it would have already been detected. It is believed that DM can interact weakly if it is composed of weakly interacting particles [3], though there is no evidence to support this idea. So far, observations indicate that DM acts through gravitational interactions and seems to behave frictionless. Due to this frictionless behavior, DM is predicted by N-body simulations to be distributed in spherically symmetric halos [4].

To investigate the distribution of DM within any galaxy a number of different phenomenological density profiles have been proposed in the literature [5]:

- Cored profiles with central density  $\rho_0$  and scale radius  $r_0$  with  $x = r/r_0$  being the dimensionless radial distance (coordinate) from the center of a galaxy to the considered point:

– pseudo-isothermal (ISO) sphere profile:

$$\rho_{Iso}(r) = \frac{\rho_0}{1+x^2}, \quad (1)$$

– Burkert profile:

$$\rho_{Bur}(r) = \frac{\rho_0}{(1+x)(1+x^2)}. \quad (2)$$

• Cusped profiles with characteristic radius  $r_0$  where the density profile has a logarithmic slope of  $-2$  (the “isothermal” value) and  $\rho_0$  as the local density at that radius.

– Navarro–Frenk–White profile:

$$\rho_{NFW}(r) = \frac{\rho_0}{x(1+x)^2} \quad (3)$$

– Moore profile:

$$\rho_{Moo}(r) = \rho_0 x^{-1.16} (1+x)^{-1.84} \quad (4)$$

• – Einasto profile with an extra parameter  $n$  which determines the degree of curvature (shape) of the profile. The family of Einasto profiles with relatively large indices  $n > 4$  are identified with cuspy halos, while low index values  $n < 4$  presents a cored-like behavior. The lower the index  $n$ , the more cored-like the halo profile:

$$\rho_{Ein}(r) = \rho_0 \exp\left\{2n\left(1 - x^{\frac{1}{n}}\right)\right\}. \quad (5)$$

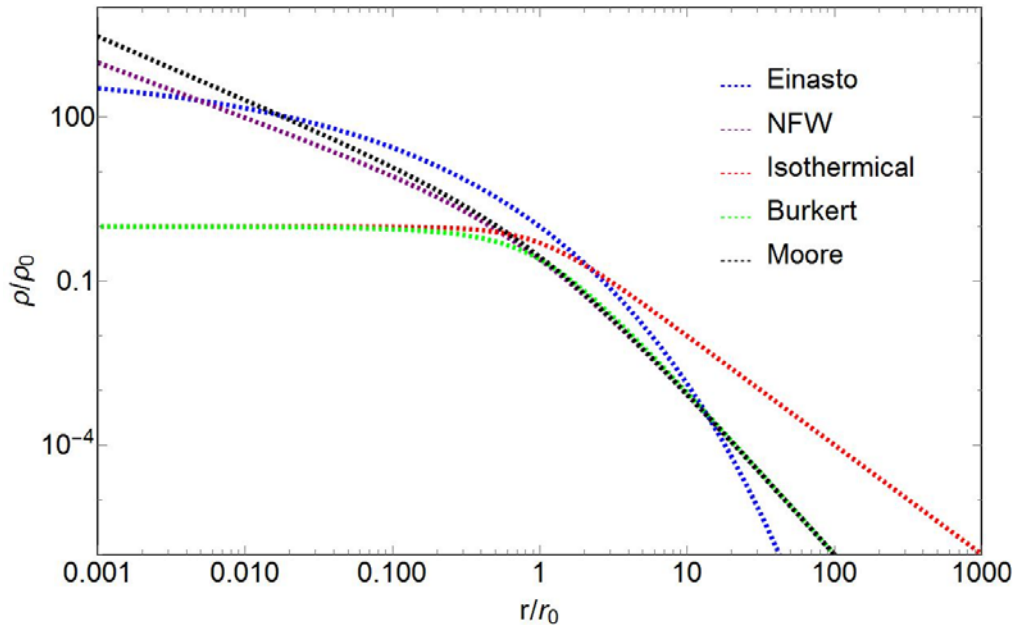


Figure 1 - Different phenomenological dark matter density profiles

In the case of Milky Way Galaxy these profiles have two constraints. They are anchored at a distance of 8.33 kilo parsec (kpc), which is the distance from the center of Milky Way Galaxy to the Sun. The second constraint is the total predicted mass of the distribution inside a radius of 60 kpc. This mass has been predicted to be  $M = 4.7 \cdot 10^{11} M_{\odot}$ . The comparison among the profiles is shown in Figure 1. The

profiles follow a similar shape when the distance from the galactic center is larger than that of the Sun and differ more towards the center of the galaxy. The Burkert and isothermal profiles become constant and approach their characteristic density, while the NFW and Moore profiles diverge near the center.

### Methods

The problem of the DM distribution in galaxies, as usually addressed in the literature, is mainly focused in the halo regions and associated with the galaxy rotation curves obtained from the observations [6]. A galactic rotation curve describes how the rotation velocity of objects in the galaxy changes as a function of the object's distance to the center. As an example we consider a central mass with a test particle moving on a circular path in the field of the former. The rotational velocity can be determined in this example from Newton's gravitational equations and the centrifugal force:

$$F = G \frac{M(r) \cdot m}{r^2} = \frac{m \cdot v^2(r)}{r} \Rightarrow v(r) = \sqrt{\frac{GM(r)}{r}} \quad (6)$$

where  $M(r)$  is the central mass profile,  $m$  is the test mass and  $r$  is the distance between the central mass and the test mass. The rotational velocity is represented by  $v(r)$ .

The mass of the galaxy is not distributed in a central point, so one has to consider the actual distribution. The calculation for the galactic distribution requires the integration of Newton's gravitational equations with the entire distribution taken into account. We adopt a circular motion of a test mass around the center of the galaxy. The expected rotation curve would then increase quickly since the considered mass increases rapidly, due to the high density near the center. Based on the visible mass, the rotation curve is expected to eventually drop off near the edge of the galaxy like  $\frac{1}{\sqrt{r}}$  as in formula (6). This is

however not what is measured in astronomy. The rotation curves do not drop off according to Newton's laws but stay flat near the edge of the galaxies [7]

In equation (6) we calculate the mass profile  $M(r)$  with the help of the following formula:

$$M(r) = \int_0^r \rho(r') \cdot 4\pi r'^2 dr' \quad (7),$$

where  $\rho(r)$  is the DM density profile taken from Eqs. (1) through (5).

For convenience, we choose such units where the mass is given in the units of one solar mass and the radial distance is in parsecs:

$$v(r) = 10^{-5} \sqrt{\frac{G \cdot M(r) \cdot M_{sun}}{r \cdot pc}} \quad (8)$$

where  $M_{sun} = M_{\odot}$  is the mass of the Sun in grams,  $pc$  is parsec in cm, and the numerical factor in front of the square root converts the units of  $v(r)$  into km/s.

In order to carry out the fitting procedure we exploit the Levenberg-Marquardt nonlinear least squares method [8, 9].

### Results

We compare the fits of rotation curves obtained by means of the models considered in the previous section. Since one has to compare the models with different number of parameters, which are not nested into each other, we use the Bayesian Information Criterion (BIC) formulated and developed by Schwarz [10]. It provides a penalty to models with larger number of parameters to check which of them is more likely to be realistic. A model with a minimum BIC value is favored [5]. The results of the fitting procedure are presented in Tables 1 - 6 and in Figs. 2 - 7.

Table 1 - Model parameters for irregular dwarf galaxy DDO 154

The mass of the baryonic (luminous) matter in the galaxy is $3.58 \cdot 10^8 M_{\odot}$ [11]					
Profiles	$\rho_0 \pm \delta\rho_0, 10^{-3} \frac{M_{\odot}}{pc^3}$	$r_0 \pm \delta r_0, \text{ kpc}$	$M \pm \delta M, M_{\odot}$	$n$	BIC
Burkert	$32.74 \pm 1.47$	$2.44 \pm 0.07$	$(7.59 \pm 0.61) \cdot 10^8$	-	149
NFW	$1.61 \pm 0.35$	$14.46 \pm 2.41$	$(1.18 \pm 0.49) \cdot 10^{10}$	-	207
ISO	$34.74 \pm 1.89$	$1.31 \pm 0.05$	$(2.07 \pm 0.22) \cdot 10^8$	-	141
Moore	$0.31 \pm 0.18$	$38.96 \pm 18.21$	$(5.23 \pm 6.14) \cdot 10^{10}$	-	235
Einasto	$2.73 \pm 0.27$	$4.53 \pm 0.25$	$(2.14 \pm 0.33) \cdot 10^9$	$1.72 \pm 0.13$	119

As one can see from table 1, for DDO 154 galaxy the BIC value is minimum for the Einasto profile and is maximum for the Moore profile. The mass obtained by means of the Einasto profile is one order of magnitude larger than the visible mass.

Table 2 - Model parameters for spiral galaxy NGC 1560

The mass of the baryonic matter in the galaxy is $8.2 \cdot 10^8 M_{\odot}$ [12]					
Profiles	$\rho_0 \pm \delta\rho_0, 10^{-3} \frac{M_{\odot}}{pc^3}$	$r_0 \pm \delta r_0, \text{ kpc}$	$M \pm \delta M, M_{\odot}$	$n$	BIC
Burkert	$47.81 \pm 2.71$	$3.12 \pm 0.12$	$(2.32 \pm 0.24) \cdot 10^9$	-	142
NFW	$2.61 \pm 0.47$	$17.32 \pm 2.38$	$(3.31 \pm 1.14) \cdot 10^{10}$	-	136
ISO	$47.11 \pm 2.93$	$1.76 \pm 0.08$	$(6.98 \pm 0.85) \cdot 10^8$	-	130
Moore	$0.54 \pm 0.22$	$43.81 \pm 13.96$	$(1.32 \pm 1.06) \cdot 10^{11}$	-	140
Einasto	$1.75 \pm 1.28$	$9.36 \pm 4.09$	$(1.32 \pm 1.57) \cdot 10^{10}$	$2.86 \pm 1.00$	135

For NGC 1560 galaxy the BIC value is minimum for the isothermal profile and is maximum for the Burkert profile, though the difference between the values is not large. It is worth noting that the modest improvement in the BIC of the isothermal sphere model with respect to the Einasto and NFW is not that strong to assess that the isothermal profile has to be preferred.

Table 3 - Model parameters for intermediate spiral galaxy NGC 2403

The mass of the baryonic matter in the galaxy is $2.58 \cdot 10^9 M_{\odot}$ [11]					
Profiles	$\rho_0 \pm \delta\rho_0, 10^{-3} \frac{M_{\odot}}{pc^3}$	$r_0 \pm \delta r_0, \text{ kpc}$	$M \pm \delta M, M_{\odot}$	$n$	BIC
Burkert	$207.94 \pm 10.16$	$2.77 \pm 0.07$	$(7.06 \pm 0.51) \cdot 10^9$	-	1252
NFW	$32.64 \pm 1.11$	$6.91 \pm 0.13$	$(2.62 \pm 0.14) \cdot 10^{10}$	-	764
ISO	$521.34 \pm 22.83$	$0.84 \pm 0.02$	$(8.27 \pm 0.6) \cdot 10^8$	-	842
Moore	$15.66 \pm 0.57$	$9.41 \pm 0.18$	$(3.79 \pm 0.21) \cdot 10^{10}$	-	732
Einasto	$4.35 \pm 0.43$	$9.43 \pm 0.48$	$(3.76 \pm 0.56) \cdot 10^{10}$	$5.98 \pm 0.27$	692

For NGC 2403 galaxy the BIC value is minimum for the Einasto profile and is maximum for the Burkert profile. The mass obtained by the Einasto profile is one order of magnitude larger than the visible mass.

Table 4 - Model parameters for unbarred spiral galaxy NGC 2976

The mass of the baryonic matter in the galaxy is $1.36 \cdot 10^8 M_{\odot}$ [11]					
Profiles	$\rho_0 \pm \delta\rho_0, 10^{-3} \frac{M_{\odot}}{pc^3}$	$r_0 \pm \delta r_0, \text{ kpc}$	$M \pm \delta M, M_{\odot}$	$n$	BIC
Burkert	$273.17 \pm 12.6$	$1.7 \pm 0.08$	$(2.14 \pm 0.24) \cdot 10^9$	-	126
NFW	$0.77 \pm 3.73$	$138.45 \pm 664.57$	$(0.49 \pm 5.61) \cdot 10^{13}$	-	174
ISO	$238.66 \pm 11.52$	$1.07 \pm 0.05$	$(7.91 \pm 1.04) \cdot 10^8$	-	129
Moore	$0.05 \pm 2.1$	$758.54 \pm 3040.75$	$(0.06 \pm 2.72) \cdot 10^{15}$	-	202
Einasto	$35.5 \pm 12.3$	$2.52 \pm 0.61$	$(4.39 \pm 2.72) \cdot 10^9$	$1.1 \pm 0.3$	128

For NGC 2976 galaxy the BIC value is minimum for the Burkert profile and is maximum for the Moore profile. As before the small difference in the BIC with respect to the Einasto, isothermal and Burkert profiles does not allow to assess which model is better (they are comparable with each other). For this galaxy the mass inferred by the Burkert profile is ten times larger than the visible mass.

Table 5 - Model parameters for spiral galaxy NGC 3627

The mass of the baryonic matter in the galaxy is $8.18 \cdot 10^8 M_{\odot}$ [11]					
Profiles	$\rho_0 \pm \delta\rho_0, 10^{-3} \frac{M_{\odot}}{pc^3}$	$r_0 \pm \delta r_0, \text{ kpc}$	$M \pm \delta M, M_{\odot}$	$n$	BIC
Burkert	$2660 \pm 477$	$1.16 \pm 0.09$	$(6.61 \pm 0.24) \cdot 10^9$	-	53
NFW	$1670 \pm 498$	$1.47 \pm 0.21$	$(1.28 \pm 0.53) \cdot 10^{10}$	-	60
ISO	$43938 \pm 148672$	$0.13 \pm 0.22$	$(2.57 \pm 7.79) \cdot 10^{10}$	-	86
Moore	$1087 \pm 343$	$1.71 \pm 0.24$	$(1.57 \pm 0.69) \cdot 10^{10}$	-	61
Einasto	$147.4 \pm 9.9$	$2.71 \pm 0.11$	$(2.21 \pm 0.25) \cdot 10^{10}$	$1.04 \pm 0.13$	30

For NGC 3627 galaxy the BIC value is minimum for the Einasto profile and is maximum for the isothermal profile. Here the mass inferred by the Einasto profile is one order of magnitude larger than the visible mass.

Table 6 - Model parameters for spiral galaxy NGC 5585

The mass of the baryonic matter in the galaxy is $1.6 \cdot 10^9 M_{\odot}$ [13]					
Profiles	$\rho_0 \pm \delta\rho_0, 10^{-3} \frac{M_{\odot}}{pc^3}$	$r_0 \pm \delta r_0, \text{ kpc}$	$M \pm \delta M, M_{\odot}$	$n$	BIC
Burkert	$89.6 \pm 2.3$	$2.83 \pm 0.05$	$(3.24 \pm 0.14) \cdot 10^9$	-	38
NFW	$6.02 \pm 1.4$	$12.56 \pm 2.02$	$(2.89 \pm 1.2) \cdot 10^{10}$	-	76
ISO	$90.5 \pm 4.5$	$1.52 \pm 0.05$	$(8.57 \pm 0.82) \cdot 10^8$	-	51
Moore	$1.79 \pm 0.77$	$23.69 \pm 7.27$	$(6.93 \pm 4.85) \cdot 10^{10}$	-	81
Einasto	$10.26 \pm 0.61$	$4.48 \pm 0.12$	$(7.3 \pm 0.6) \cdot 10^9$	$1.27 \pm 0.08$	33

For NGC 5585 galaxy the BIC value is minimum for the Einasto profile and is maximum for the Moore profile. Here as before the BIC is similar between the Einasto and Burkert models. The mass inferred by the Einasto profile has the same order as the visible mass.

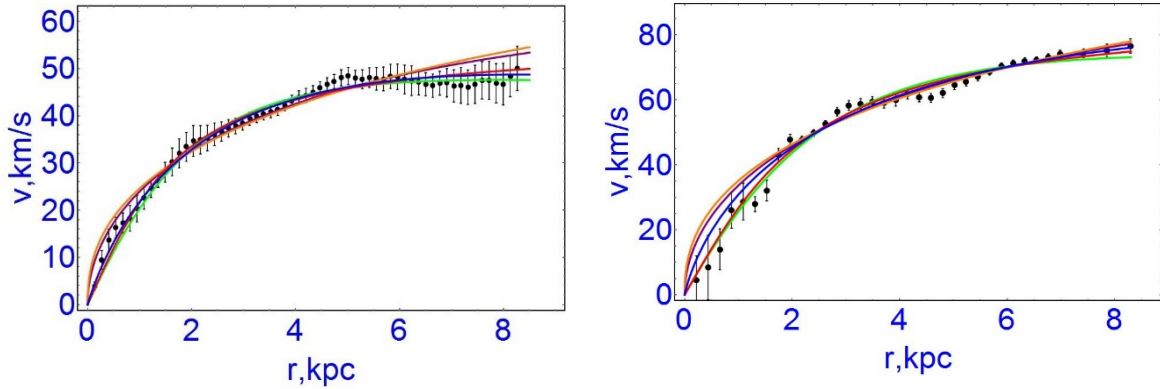


Figure 2 - Rotation curves of galaxies and fitted models.  
Left panel: galaxy DDO 154. Right panel: galaxy NGC 1560

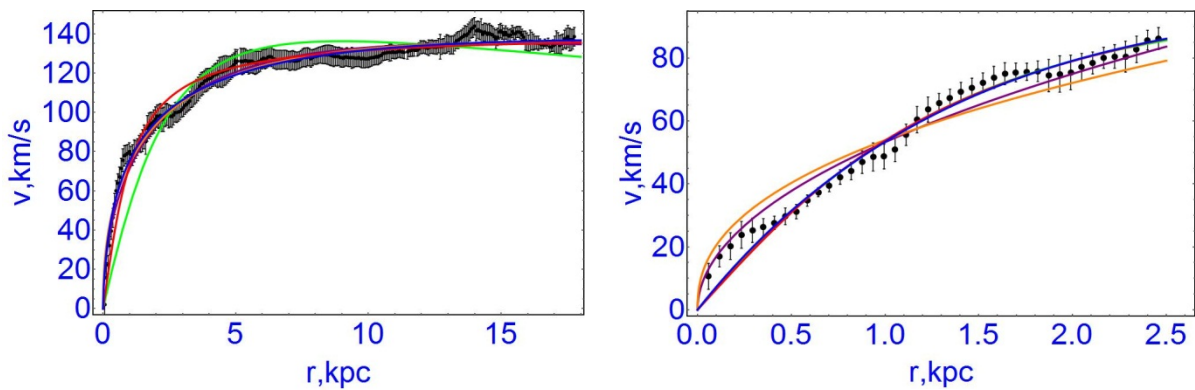


Figure 3 - Rotation curves of galaxies and fitted models.  
Left panel: galaxy NGC 2403. Right panel: galaxy NGC 2976

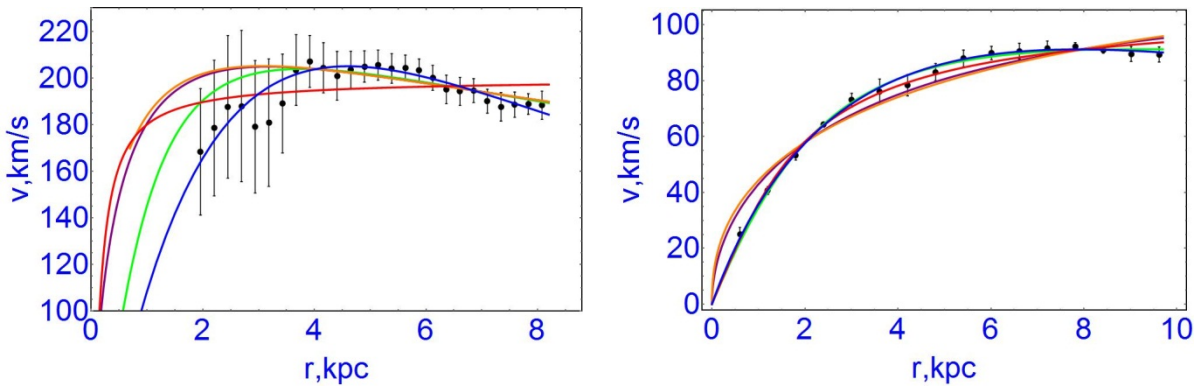


Figure 4 - Rotation curves of galaxies and fitted models.  
Left panel: galaxy NGC 3627. Right panel: galaxy NGC 5585.

In figures 2-4 the black thick points show observational data with their error bars for one dwarf and five spiral galaxies, the green curves show the Burkert profile, the purple curves show the NFW profile, the red curves show the isothermal profile, the orange curves show the Moore profile and the blue curves show the Einasto profile (color online). The theoretical curves were obtained by the fitting procedure. Using the method of least squares we calculated the numerical values of the scale radius and characteristic density. In the case of the Einasto profile, the value of the Einasto index was also obtained. In the end we calculated the mass of DM in the galaxies.

### Discussion and Conclusion

We have analyzed one dwarf galaxy and five spiral galaxies in this work. The complex structure of galaxies was abandoned and the DM distribution was adopted to be spherical for a given galaxy. The rotation curves constructed in this work have been compared with the analogous results in the literature for galaxies NGC 2403, NGC 3627, NGC 2976, DDO 154 in Ref. [11], and for galaxies NGC 1560 and NGC 5585 in Refs. [12] and [13], respectively.

The model parameters were inferred from the observational data points by using “NonLinearModelFit” command in the scientific software “Wolfram Mathematica 11”. The command allows one to automatically conduct the fitting procedure for a given model and data points. As a result, the total mass of DM was estimated in the considered galaxies and confronted with their luminous masses. The DM mass, in many cases, is larger than the visible mass, as expected.

The Einasto model showed the best results in four cases (DDO154, NGC 2403, NGC 3627, NGC 5585), Burkert and Isothermal profiles showed good results for NGC 2976 and NGC 1560 galaxies, respectively, as the BIC value was the lowest compared to other models. Unlike other models, the Einasto model depends upon three parameters and one gets a better fit. Therefore, there is a higher compliance with the observations. The NFW profile showed small deviations from the observed galaxies NGC 5585, NGC 1560, NGC 2976. In other profiles we have no noticeable differences.

Overall, all models considered in this work showed good results, though in some cases not all the data points were covered with the theoretical curves. These discrepancies can be caused by the fact that we simply ignored the complex structure, the baryonic constituents in galaxies. If we took into account the inner structure of galaxies as in Ref. [14] and constituents of the matter as in Ref [15], probably the fits would be much better than the ones presented in this work.

Nevertheless there are still a plenty of open issues related to DM. Although one can observe indirectly the presence of DM in any galaxy or clusters, we still do not know why the DM distribution is so different from one galaxy to another. For example, the recent discovery of DM distribution in the Markarian galaxy shows that DM is mainly concentrated in the core of the galaxy [16]. Another example shows a galaxy with barely no DM [17].

The nature of DM particles still remains mystery, though there are some theoretical models predicting the whole set of DM particles, see Refs. [3, 18] for details. The role of DM in the evolution of the universe is yet to be understood.

It will be interesting to investigate other galaxies [19], taking into account their intricate structure, and involving latest theoretical models. This issue will be addressed in future studies.

### Acknowledgement

The work was supported by the MES of the RK, Program 'Center of Excellence for Fundamental and Applied Physics' IRN: BR05236454. K.M. expresses her deep gratitude to F. Walter for providing the observational data points of rotation curves for the six galaxies considered in this work. M.M. is fully supported by INFN as part of the MoonLIGHT-2 experiment in the framework of the research activities of CSN2.

### APPENDIX

The rotation curve data points for galaxies NGC 2403, NGC 3627, NGC 2976, DDO 154 are given in Ref. [11], and for galaxies NGC 1560, NGC 5585 are taken from [12] and [13], respectively.

In the observational data, the distance from the center to the point  $R$  is represented in angular seconds. 1 angular second is equal to  $\frac{1}{3600}$  part of a degree. To convert an angular second into a kiloparsec, one should use the following general formula:

$$R = a \cdot \text{tg}(\varphi) \quad (9)$$

where  $\varphi$  is the specified distance in angular seconds,  $a$  is the distance between our galaxy (Earth) and the galaxy under consideration. We express  $\varphi$  in radians. Finally for  $R$  we obtain:

$$R = a \cdot \operatorname{tg} \left( \frac{1}{3600} \cdot \frac{\pi}{180^\circ} \varphi \right) \quad (10)$$

Table 7 - The distance between Milky Way Galaxy (Earth) and the galaxy under consideration

Galaxies	$a$ , [kpc]	References
DDO 154	4300	[11]
NGC 1560	3000	[12]
NGC 5585	6200	[13]
NGC 2403	3180	[20]
NGC 3627	10100	[21]
NGC 2976	3450	[22]

ӘОЖ 524.7, 524-1:629.78

ХҒТАР 41.27.29, 89.51.17

**К. Бошкаев<sup>1,2,3</sup>, Г. Жумаханова<sup>2</sup>, К. Муталипова<sup>2</sup>, М. Муччино<sup>4</sup>**

<sup>1</sup>АТҰНЗ, <sup>2</sup>Әл-Фараби атындағы Қазақ Ұлттық Университеті, Алматы, Қазақстан

<sup>3</sup>Физика кафедрасы, Назарбаев Университеті, Нұр-Сұлтан, Қазақстан

<sup>4</sup>ҰЯФИ, Фраскати Ұлттық Лабораториясы, Фраскати, Италия

#### ҚАРАҢҒЫ МАТЕРИЯНЫҢ ӘР ТҮРЛІ ПРОФИЛЬДЕРІН ЗЕРТТЕУ

**Аннотация.** Әр түрлі галактикалардағы қараңғы материяның массасы таралуын бағалау үшін әдебиетте белгілі, кеңінен пайдаланылатын Изотермал, Буркерт, Наварро-Френк-Уайт, Мур және Эйнасто профильдері қолданылады. Ньютонның гравитация теориясы ауқымды галактикалық масштабтардағы есептеулерді орындау үшін жұмылдырылды. Алуан түрлі галактикаларда қараңғы материяның таралуы (үлестірілуі) сфералық деп ұйғарылды және галактикалардың күрделі құрылымы, яғни олардың ядросы, ішкі және сыртқы балдждары, дискілері мен галолары ескерілмеді. Теориялық айналу қисықтары галактикалар үшін бақылау мәліметтерімен сәйкестендірілді. Ең кіші квадраттар әдісі көмегімен үлгілердің параметрлері бақылау деректерінен есептеліп алынды және неғұрлым сәйкес келетін үлгіні анықтау үшін Байестік Информациялық Критерий қолданылды. Қараңғы материяның массасы барлық көрсетілген профильдер арқылы әр дербес галактика үшін есептелінді және галактикалардың көрінетін массасымен салыстырылады. Нәтижелер әдебиеттегі мәліметтерімен сәйкес келеді.

**Түйін сөздер:** галактикалар, айналу қисықтары, қараңғы материя.

УДК 524.7, 524-1:629.78

МРНТИ 41.27.29, 89.51.17

**К. Бошкаев<sup>1,2,3</sup>, Г. Жумаханова<sup>2</sup>, К. Муталипова<sup>2</sup>, М. Муччино<sup>4</sup>**

<sup>1</sup>ННЛОТ, <sup>2</sup>Казахский Национальный Университет им. аль-Фараби, Алматы, Қазақстан

<sup>3</sup>Кафедра физики, Назарбаев Университет, Нур-Султан, Қазақстан

<sup>4</sup>НИЯФ, Национальная Лаборатория Фраскати, Фраскати, Италия

#### ИССЛЕДОВАНИЕ РАЗЛИЧНЫХ ПРОФИЛЕЙ ТЕМНОЙ МАТЕРИИ

**Аннотация.** Различные, общепринятые и широко используемые феноменологические профили темной материи, такие как псевдоизотермическая сфера, профили Буркерта, Наварро-Френка-Уайта, Мура и Эйнасто, используются для оценки распределения массы темной материи в различных галактиках. Ньютонская гравитация используется для выполнения вычислений в больших галактических масштабах. Распределение темной материи в различных типах галактик предполагается сферическим без учета сложной структуры галактик, таких как их ядра, внутренние и внешние балджи, диски и гало. Теоретические кривые вращения сопоставлены с наблюдениями для каждой галактики. Посредством алгоритма наименьших квадратов параметры модели выводятся из данных наблюдений и подвергаются Байесовскому информационному критерию, который определяет более предпочтительную модель. Массы темной материи



рассчитываются для каждой галактики со всеми перечисленными профилями и сравниваются с видимыми массами галактик. Результаты согласуются с данными в литературе.

**Ключевые слова:** галактики, кривые вращения, темная материя.

**Information about authors:**

Boshkayev Kuantay - PhD in Theoretical Physics and PhD in Relativistic Astrophysics, Associate Professor at the Department of Theoretical and Nuclear Physics, KazNU, Research Associate at NNLOT, KazNU, Almaty, Kazakhstan, <http://orcid.org/0000-0002-1385-270X>

Muccino Marco - PhD in Relativistic Astrophysics, Research Associate at INFN, Laboratori Nazionali Di Frascati, Frascati, Italy <http://orcid.org/0000-0002-2234-9225>

Zhumakhanova Gulnur - 2 year PhD student at the Department of Theoretical and Nuclear Physics, KazNU, Almaty, Kazakhstan <https://orcid.org/0000-0003-1346-3875>

Mutalipova Kalbinur - 1 year master student at the Department of Theoretical and Nuclear Physics, KazNU, Almaty, Kazakhstan, <http://orcid.org/0000-0003-0226-132X>

**REFERENCES**

- [1] Milgrom M. (1983) A modification of the Newtonian dynamics as a possible alternative to the hidden mass hypothesis, *The Astrophysical Journal*, 270:365-370. DOI: 10.1086/161130
- [2] Blioh P.V., Minakov A.A. (1990) Gravitational lenses [Gravitatsionnyye linzy]. Kiev, Russia. ISBN: 5-07-001197-9
- [3] Steigman G., Turne M.S. (1985) Cosmological constraints on the properties of weakly interacting massive particles, *Nuclear Physics B*, 253:375-386. DOI: 10.1016/0550-3213(85)90537-1
- [4] Cirelli M, Gennaro C. (2011) PPPC 4 DM ID : A Poor Particle Physicist Cookbook for Dark Matter Indirect Detection, *JCAP*, 2011. DOI: 10.1088/1475-7516/2011/03/051
- [5] Siutsou I., Argüelles C.R., Ruffini R. (2015) Dark Matter Massive Fermions and Einasto Profiles in Galactic Haloes, *Astronomy Reports*, 59:656-666. DOI: 10.1134/S1063772915070124
- [6] Einasto J. (2013) Dark Matter, *Brazilian Journal of Physics*, 43:369-374. DOI: 10.1007/s13538-013-0147-9
- [7] Marchesini D., Elena D'Onghia, Chincarini G., Claudio F. (2002)  $H\alpha$  rotation curves: the soft core question, *The Astrophysical Journal* 575: 801-813. DOI: 10.1086/341475
- [8] Levenberg K. (1944) A method for the solution of certain non-linear problems in least squares, *Quarterly of Applied Mathematics*, 2:164-168. DOI: 10.1090/qam/10666
- [9] Marquardt D. (1963) An algorithm for least-squares estimation of nonlinear parameters, *SIAM Journal on applied mathematics*, 11: 431-441. DOI: 10.1137/0111030
- [10] Schwarz G. (1978) Estimating the Dimension of a Model, *Institute of Mathematical Statistics*, 6:461-464. DOI: 10.1214/aos/1176344136
- [11] Walter F., Brinks E., de Blok, Bigiel F., Kennicutt R., Leroy A. (2008) THINGS: the hi nearby galaxy survey, *The Astrophysical Journal*, 136: 2563-2647. DOI: 10.1088/0004-6256/136/6/2563
- [12] Broeils AH (1992) The mass distribution of the dwarf spiral galaxy NGC 1560, *Astronomy and astrophysics*, 256:19-32. ISSN: 0004-6361 (it does not have DOI)
- [13] Stéphanie C., Carignan C. (1991) A Dark-Halo-Dominated Galaxy: NGC 5585, *The Astronomical Journal*, 102:904-915. DOI: 10.1086/115922
- [14] Sofue Y. (2015) Dark halos of M31 and the Milky Way, *Astronomical Society of Japan*, 67(4), 75(1-9). DOI: 10.1093/pasj/psv042
- [15] Salucci P. (2018) Dark matter in galaxies: evidences and challenges, *Foundations of Physics*, 48:1517-1537. DOI: 10.1007/s10701-018-0209-5
- [16] David A. Buote, Aaron J. Barth. (2019) The extremely high dark matter halo concentration of the relic compact elliptical galaxy Mrk 1216, *The Astrophysical Journal*, 877:91. DOI: 10.3847/1538-4357/ab1008
- [17] Danieli S., Pieter van Dokkum, Conroy C. (2019) Still missing dark matter: KCWI high-resolution stellar kinematics of NGC 1052-DF2, *The Astrophysical Journal Letters*, 874:12. DOI: 10.3847/2041-8213/ab0e8c
- [18] Merle A. (2013) keV Neutrino model building, *International Journal of Modern Physics D*, 22. DOI: 10.1142/S0218271813300206
- [19] Denisyyuk E.K., Valiullin R.R. (2019) Rotating curve of the galaxy NGC 1068, *News of the National Academy of Sciences of The Republic of Kazakhstan. Physico-Mathematical Series. Vol. 3, No. 325, P. 153 - 157. ISSN 1991-346X. <https://doi.org/10.32014/2019.2518-1726.34>*
- [20] Fraternali F., Sancisi R., Tom Oosterloo (2002) Deep HI Survey of the spiral galaxy NGC 2403, *The Astronomical Journal*, 123: 3124-3140. DOI: 10.1086/340358
- [21] Macri L.M., Stetson P.B., Bothun G.D., Jha S. (2001) The discovery of cepheids and a new distance to NGC 2841 using the Hubble space telescope, *The Astrophysical Journal*, 559:243-259. DOI: 10.1086/322395
- [22] Joshua J.Adams., Gebhardt K., Hill G.J. (2003) High-resolution measurements of the dark matter halo of NGC 2976: Evidence for a shallow density profile, *The Astrophysical Journal*, 596: 957-981. DOI: 10.1086/378200